Electronic Transport Properties or Ensembles of Perylene-Substituted Poly-isocyanopeptide Arrays

Finlayson, Christopher Edward; Friend, Richard H.; Otten, Matthijs B. J.; Schwartz, Erik; Cornelissen, Jeroen. J. L. M.; Nolte, Roeland. L. M.; Rowan, Alan E.; Samori, Paolo; Palermo, Vicenzo; Liscio, Andrea; Peneva, Kalina; Muellen, Klaus; Trapani, Sara; Beljonne, David

Published in:
Advanced Functional Materials

DOI:
10.1002/adfm.200800943

Publication date:
2008

Citation for published version (APA):
Finlayson, C. E., Friend, R. H., Otten, M. B. J., Schwartz, E., Cornelissen, J. J. L. M., Nolte, R. L. M., Rowan, A. E., Samori, P., Palermo, V., Liscio, A., Peneva, K., Muellen, K., Trapani, S., & Beljonne, D. (2008). Electronic Transport Properties or Ensembles of Perylene-Substituted Poly-isocyanopeptide Arrays. *Advanced Functional Materials*, *18*(24), 3947-3955. https://doi.org/10.1002/adfm.200800943

Submitted to ADVANCED FUNCTIONAL MATERIALS

DOI: 10.1002/adfm.((please add manuscript number))

Electronic transport properties of ensembles of perylene-substituted poly-isocyanopeptide arrays**

By C.E. Finlayson, R.H. Friend, M.B.J. Otten, E. Schwartz, J.J.L.M. Cornelissen, R.J.M. Nolte, A.E. Rowan, P. Samorì, V. Palermo, A. Liscio, K. Peneva, K. Müllen, S. Trapani, and D. Beljonne*

[*] Dr C.E. Finlayson, Prof R.H. Friend
Cavendish Laboratory, JJ Thomson Avenue,
Cambridge CB3 0HE (UK)

E-mail: cef26@cam.ac.uk

M.B.J. Otten, E. Schwartz, Dr J.J.L.M. Cornelissen, Prof R.J.M. Nolte, Prof A.E. Rowan
Institute for Molecules and Materials,
Radboud University Nijmegen,
Toernooiveld 1, 6525 ED Nijmegen (Netherlands)

Dr P. Samorì[#], Dr V. Palermo, Dr A. Liscio
Istituto per la Sintesi Organica e la Fotoreattività,
Consiglio Nazionale delle Ricerche,
via Gobetti 101, 40129 Bologna (Italy)

Dr K. Peneva, Prof K. Müllen
Max-Planck Institute for Polymer Research
Ackermannweg 10, 55124 Mainz (Germany)

S. Trapani, Prof D. Beljonne
Université de Mons-Hainaut
Place du Parc, 20
7000 Mons (Belgium)

[**] This work was supported by the ESF-SONS2-SUPRAMATES project, the Regione Emilia-Romagna PRIITT Nanofaber Net-Lab, the ERA-Chemistry project SurConFold, and the EU through the projects Marie Curie EST - SUPER (MEST-CT-2004-008128), the RTN PRAIRIES (MRTN-CT-2006-035810), and ForceTool (NMP4-CT-2004-013684). The work in Nijmegen was supported by the Netherlands Organization for scientific research chemistry section (top grant for R.J.M.N and V.I.C.I, A.E.R), Nanoned STW (A.E.R.) and the Royal Netherlands Academy for Arts and Sciences (KNAW). The work in Mons is partly supported by the Interuniversity Attraction Pole program of the Belgian Federal Science Policy Office (PAI 6/27) and by FNRS-FRFC. DB is research director of FNRS. S.T. acknowledges a grant from « Fonds pour la Formation à la Recherche dans l'Industrie et dans l'Agriculture (FRIA) ». C.E.F. thanks Dr C.R. Newman and Dr R. Shikler of the Cavendish Laboratory, and also *Cambridge Display Technology Ltd*, for help and advice.

[#]Also at- Nanochemistry Laboratory
ISIS – CNRS 7006,

Submitted to ADVANCED FUNCTIONAL MATERIALS

Université Louis Pasteur,
8, allée Gaspard Monge, 67000 Strasbourg (France)

Keywords: poly-isocyanides, macromolecules, perylene-diimide, field-effect transistors, electronic transport

The electronic transport properties of stacks of perylene-bis(dicarboximide) (PDI) chromophores, covalently fixed to the side arms of rigid, helical polyisocyanopeptides, are studied using thin-film transistors (TFTs). In device architectures where the transistor channel lengths are somewhat greater than the average polymer chain length, we find carrier mobilities of order 10^{-3} cm^2/Vs at 350K, which are limited by inter-chain transport processes. The influence of π-π interactions on the material properties is studied by using PDIs with and without bulky substituents in the bay area. In order to attain a deeper understanding of both the electronic and the electronic-transport properties of these systems, we combine studies of self-assembly on surfaces with electronic characterization using Kelvin Probe Force Microscopy (KFPM), and also a theoretical study of electronic coupling. The use of a rigid polymer backbone as a scaffold to achieve a full control over the position and orientation of functional groups is of general applicability and interest in the design of building blocks for technologically important functional materials, as well as in more fundamental studies of chromophoric interactions.

1. Introduction

Achieving a full control over the chromophore-chromophore interaction in π-conjugated macromolecular architectures across multiple length scales is a fundamental requirement for the tuning of their optical and electronic properties, and ultimately for their complete exploitation in opto- and nano-electronics devices.[1-3]

While the bottom-up growth from both solution and vacuum deposition of highly ordered multi-chromophoric structures with size in the range 1-10 nm can be achieved by mastering non-covalent interactions such as π–π stacking, the fabrication of larger supramolecular structures with inter-chromophoric interactions at will is more challenging. Such a goal can be accomplished by utilization of the self-assembly of molecules[4] or by using pre-patterned surfaces and structures to drive the order on macroscopic scale.[5,6] However, in this latter case the controlled organization across multiple length scales obtained through the modulation of the complex interplay between short-range intermolecular interactions and long-range interfacial interaction does not represent an easy task.

A much more viable approach involves the use of molecular “scaffolding”, i.e. the exploitation of a hundreds of nanometers long anisotropic nano-object with a pre-programmed structure, as a backbone to position functional groups in specific location. Using this strategy the chromophore-chromophore interaction can be controlled from the sub-nanometer up to the several hundreds of nanometers scale. This has paved the way towards the fabrication of organic based microelectronic devices, such as LEDs,[7,8] field-effect[9] and light emitting transistors,[10] flexible displays[11] and solar cells,[12-14] with improved performance.

In this paper, we have focused on the use of poly-isocyanodipeptides[15] as scaffolds with which to tailor inter-chromophore interactions among perylene dyes covalently linked to the aliphatic side-chains. These polymeric systems have been synthesized via a nickel catalysed polymerisation reaction of isocyanide monomers, as described in detail elsewhere.[16-18] The polymer chains are ultra-stiff, as shown by a persistence length as high as 76 nm, and can have a contour length exceeding 12 μm.[19] The side chains of this polymers can be functionalized with various moieties such as carboxyl units, thiophene[20] or perylene-bis(dicarboximide)(PDI),[21,22] thereby offering control of spatial position over hundreds of nanometers. This approach offers a unique possibility to study the supramolecular interactions of small chromophores (perylenes, thiophenes, porphyrins etc.) interacting with each other while they are kept "in position" due to the presence of the polymeric backbone. The ability to control the stacking of chromophoric units, such as PDI, appears very interesting as a way of enhancing charge transfer in pre-designed channels for photovoltaic device applications; hence, emulating many of the vectorially directed charge-transport arrays seen in biological systems.[23]

The overall chemical structure of this kind of system involves a rigid backbone, a flexible linker, a chromophore and side alkyl functionalization; these primarily govern the mechanical properties, chromophore-chromophore interaction, optical/electronic properties and solubility of the architecture, respectively. Subtle changes in any of these four different components can lead to a dramatic change in the overall properties of the system. In particular, it is important to understand how the bay-area substitution of the perylene side chromophores can play a role in the ordering and π-π stacking of these groups, how this stacking will influence the overall morphology of the material when deposited in thin layers, and how these different

morphologies will influence both the electronic and the electronic transport properties of the thin film.

We present a comparative study of three different poly-isocyanopeptide based polymers, featuring diverse intra- and inter-molecular interactions (**Fig. 1**). Polymer P1 consists of a central poly-isocyanide (PIC) backbone bearing alanine-alanine segment and a terminal O-Me groups; the synthesis and characterization of this material has been previously reported in reference [16]. In polymer P2, perylene-bis(dicarboximide) side units are attached to the central backbone. Each PDI is optically active, but cannot interact by π-π stacking with adjacent PDIs due to the presence of bulky phenoxy substituents. Finally, polymer P3 incorporates PDIs without bulky substituents, where the only functionalization present is an alkyl side chain, in order to enhance solubility in organic solvents, thus π-π interactions between different PDIs can take place. When deposited onto substrates such as graphite, silica or mica, our previously reported AFM studies revealed that P1 and in particular P3 form "supercoils", stabilized by strong intermolecular or long-range intramolecular interactions.[18] By contrast, P2 adsorbs on the substrate surface to form isolated fibers. P3 shows more complex behavior, characterized by strong intermolecular interactions leading to the formation of coiled structures and the ubiquitous formation of bundles, which on mica are so robust that they are resistant to hydrodynamic shear alignment. A full description of the synthesis (including NMR and FTIR analysis) and optical characterization (absorption, fluorescence and circular-dichroism) of materials P2 and P3 can be found in reference [18].

We combine studies of self-assembly on surfaces with electronic and electrochemical characterization, using Kelvin Probe Force Microscopy (KFPM) and cyclic voltammetry (CV), respectively, in order to attain a deeper understanding of these complex architectures

incorporating electronic functionality. Such ordered helical arrays also offer an interesting platform for theoretical studies of fundamental interactions between chromophores. Combined with our prototypical thin-film transistor (TFT) device characterization, we therefore explore the potential for the use of such multichromophoric structures (and subsequent "next generation" materials) in technologically relevant applications, such as opto- and nano-electronics.

2. Characterization of Electronic Properties

In order to compare the electronic properties (work-function, charge carrier type and mobility) of the three molecules under study, both macroscopic and microscopic characterization was performed, using thin-film transistors (TFTs) and Kelvin Probe Force Microscopy (KPFM). These studies also enable us to examine more extrinsic device issues, such as contact-resistance and charge injection.

TFT studies were carried out using substrates consisting of a ~300nm thick buffer layer of SiO_x on top of heavily-doped Si, acting as the gate contact (**Fig. 2** inset). Top source and drain Au electrodes, with a thickness of 30 nm, were patterned using standard photolithography techniques. Channel lengths (L) of between 2-20 μm were investigated and the devices were designed with inter-digitated electrodes, giving long device widths (W) of 10,000 μm and device capacitances of ~11nF/cm^2. The prepared patterned substrates were treated with O_2 plasma, thus removing any residual adsorbates, then with hexamethyldisilizane (HMDS) in order to promote hydrophobic wetting, if required. Thin films (~50nm) of the 3 materials were spin-coated on top of the substrates from chloroform or p-xylene solution (~1 mg/ml), giving a bottom-gate transistor architecture. AFM studies showed favorable substrate wetting properties (**Fig. 2** inset): bundles of single fibers have been observed on the SiO_x surface and

the contacting between the electrodes and the material deposited within the channel seems suitable for a good charge injection at the interface.

When tested as the active layer of a transistor, measurements showed a clear difference between P1, which had no polyaromatic groups able to give charge hopping, and P2, P3, which showed a much better transconductance (**Fig. 2**). P1 did not show any semiconducting properties (no working transistor was obtained), P2 gave working transistors, but with very low n-type mobilities, while P3, as expected, gave the best results, with linear-regime mobilities of between 10^{-6} and 10^{-5} cm^2/Vs. The electron injection properties of the source and drain Au electrodes could be significantly improved by surface treatment with a chemisorbed alkanethiol self-assembled monolayer (SAM). Previous studies have shown thiol-based SAMs to raise the effective workfunction of Au by up to 1.0 eV.[24] This approach gave a best linear-regime mobility value (for P3) in the order of 10^{-4} cm^2/Vs, an on-off ratio of ~10^5 and a sub-threshold swing of ~5V/decade, at room temperature (**Fig. 3**). Not surprisingly, we find carrier mobilities which are intermediate in magnitude between the cases of amorphous spin-coated films of perylene and single-crystal perylene transistors.[25] Kelvin Probe Force Microscopy (KPFM) of working TFTs, operating above the gate-threshold bias, provided further important information about device function.[26] In the case of P3, it was found that there was no significant interfacial charging at the electrodes, which would indicate that any residual device hysteresis is due to charge trapping in the bulk and/or at the substrate surface. Such a limitation is commonly observed in *n-type* bottom-gate organic FETs.[27]

In order to appreciate the limitations of device performance due to contact resistance at the electrodes, the gated resistance *R* was plotted as function of the device channel length (*L*) for SAM-treated TFTs of P3 (**Fig. 3** inset). *R* is calculated using a graphical method $(dV/dI)_{source-}$

$_{drain}$ from the device output curves, for when V_{gate} = +100V and hence devices are operating well above switch-on threshold, at room temperature. We expect *R* to be related to the contact resistance R_0 and film resistance R_f by the simple expression:

$$R(L) = R_0 + R_f(L) \quad , \qquad \text{Eq.1.}$$

Hence, the film resistance is proportional to the channel length and the contact resistance may be estimated from a linear fit of *R(L)*. The contact resistances were extrapolated both for devices annealed at 150°C under N_2 for 1hr, and for corresponding unannealed devices. The annealing process is observed to lead to a reduction in overall film resistivity; the gated resistance of the films is related to the slope of these *R(L)* plots by Ohm's law, assuming the accumulation layer for charge transport as being contained entirely within the thin-film of the material. However, there is little change in the contact resistance, with a value of around 5 MΩ being obtained in both cases. We can compare this with previous studies of contact resistance in bottom-gate TFTs based on high–mobility polythiophenes,[28] where values in the range of 10kΩ to 10MΩ are reported for devices of similar overall channel width and architecture. Overall, our calculations show that the effects of contact resistance reduce the measured mobilities in these devices by a factor of around 2-3. Consideration of contact resistances is likely to be critical in the application of such rigid-peptide structures in "single-strand" device configurations[29] and work to address these issues is currently in progress.

In the "multi-chromophoric" systems being studied, we expect that there are two main mechanisms by which charge can be transported; along the backbone (intra-chain) and by hopping to adjacent molecules (inter-chain). In order to better understand the relative contributions of these two processes, carrier mobility as a function of temperature was studied,

and significant differences were observed in the Arrhenius plots of n-type field-effect mobility for the P2 and P3 materials (**Fig. 4**). Prior to measurement, devices were placed under vacuum in a liquid-nitrogen cooled cryostat, heated to 360K and held at this temperature for 30 minutes to ensure stabilization of any effects due to annealing. Device characteristics were then measured as a function of temperature, with a temperature sweep rate of approximately 1 K/min. In the case of P3, two distinct regimes of temperature dependence are observed, with a low temperature activation energy of ~200 meV; at high T, a rapid increase in mobility with temperature is observed (ca. 2 orders of magnitude between room temperature and T = 360K), but with some hysteresis between the upward and downward sweep. By contrast, in the case of P2, only a single non-hysteretic activation process with a characteristic energy of around 100 meV could be observed. We note that the low temperature values of activation energy are comparable with previous studies of PDI-based transistors,[30] albeit in a situation of somewhat lower device mobilities. The invariance of contact resistance with respect to annealing in TFTs of P3, as described above, indicates that the variations in mobility at high T are unlikely to be due to changes in the metal/organic interface at the electrodes. Qualitatively, the temperature dependence in the mobility of P3 is broadly consistent with variable-range transport phenomena,[31] where long-range tunneling over small energy barriers (intra-chain) predominates at low temperature, whereas activated hopping over larger energy barriers (inter-chain) is significant at higher temperatures. We speculate that the hysteresis may be due to the partial unwinding and rewinding of the polyisocyanide helix with temperature,[18] leading to some small changes in the conformal arrangement of adjacent chains. A measured mobility of order 10^{-3} cm^2/Vs is reached at 360K, which indicates that the mobilities for purely intra-chain transport will be significantly larger than those in the present case where inter-chain hopping is a limiting factor.

We have also prepared P3 in sparse random networks, by very careful control of the substrate wetting conditions and deposition parameters, rather than in continuous films (**Fig. 2**(inset)). Due to "bias-stress" effects,[32] the device characteristics show an extreme sub-linearity in transfer, as large gating fields are applied to a network of P3, which is somewhat thinner than the usual accumulation layer in the TFT device. Work is currently in progress to produce very short-channel TFT substrates[33] where the channel length is comparable to the average P3 strand length (~400nm); the reduced dimensionality of these devices should help to eliminate bias-stress effects and also allow direct measurement of intra-chain transport.

In terms of the difference in behavior between the two materials P2 and P3, we consider this can be due to factors such as differences in morphology and in the electronic structure (HOMO-LUMO gap) at the supramolecular level. By analyzing the morphologies in thin layers (**Fig. 5**), we can see that the morphology of the two molecules follows what has already been observed on different substrates at lower concentrations. The P3 layer shown in **Fig. 5a** is composed of a continuous network, where single polymeric fibers are bundled together and have a very good contact with each other. The morphology of P2 in **Fig. 5b** is very different, giving a layer of rounded "brush-like" agglomerates. The different self-assembly behavior of P2 with respect to P3 and its shorter chain length, will thus give a much worse inter-molecular contact, which can explain the differences in charge transport observed. For completeness, AFM images of thick layers of P1, P2, P3 are shown in **Fig. 6** (b-d). Another explanation can be due to the different ability of the gold electrodes to inject charges (electrons, in the case of perylene) into the active layer. In order to better understand the charge-injection properties at the Au-electrode/P3 interface, cyclic voltammetry (CV) measurements were taken on thin-films of P3, using standard methods and conditions,[34] giving a HOMO value of -6.06eV, and a LUMO of -3.99eV. These values are some 0.2 eV lower than those reported for the perylene

monomers having similar side functionalization.[35,36] When we consider that the workfunction of Au is usually in the range of -4.7eV to -5.1eV, it may be seen that a significant barrier to majority carrier (electrons) injection exists in the TFTs and these results give strong corroboration for the crucial role the SAM treatment plays in device function.

Unfortunately, CV data were not obtained for polymer P2, due to the limited solubility of this material in the solvent (acetonitrile) used in our voltammetry cell. However, KPFM measurements performed on thick layers (**Fig. 6**) showed that P2 has a much lower WF with respect to P3, with a difference of 337 mV. A similar difference was obtained from CV measurements on perylene monomers with and without phenoxy substitutents,[36] and is due to the electron-donating character of phenoxy groups for the central perylene core. This is likely to result in adverse charge injection conditions at the electrode/P2 interface. The WF values of the three molecules have been measured on different layer thickness and on different substrates. The morphology of thick layers as measured by AFM (**Fig. 6b-d**) shows the presence of well defined fibrillar structures observed for P3, and a more isotropic layer observed for P2. The same morphology is observed on ultra-thin layers, where single fiber bundles can be resolved for P3 (**Fig.7**), while rounded, isolated objects are observed for P2 (not shown). In order to obtain quantitative measurements on ultra thin layers, where the material covers only partially the substrate, we used a recently developed deconvolution procedure,[37] which allows us to eliminate the effect of lateral broadening due to the finite AFM tip size. Upon decreasing the layer thickness, we observe that the WF differences between the three molecules become less evident, but the same trend observed on thick layers is maintained, both on SiOx and graphite substrates (**Fig. 6a**).

3. Modeling of Charge transport

Perylene diimide (PDI) molecules have been widely studied as electron transporting units,[38] and the substituted polyisocyanide structures under consideration offer an interesting platform for theoretical studies of fundamental interactions between chromophores. In a hopping regime, the charge carrier mobility scales with the square of the transfer integrals, $t_{\perp}$, between neighboring chromophores, which are very sensitive to overlap between the LUMO (for electron transport) wavefunctions and hence to the organization at the supramolecular level.[39-41]

In our simulations, the PDI chromophores (as in polymer P3) are linked to the helical polyisocyanide backbone via a short saturated spacer that was submitted to a conformational search performed at the Dreiding force-field level.[42] Based on the local minima found for the relevant torsions, all possible helical stacks were constructed, among which the most realistic conformations based on simple steric arguments were selected for further investigations. The values of the torsion angles defining the conformation of the spacer and their combination have a considerable impact on the relative arrangement of the chromophores in the resulting 3D structures. Geometric optimizations were performed on systems of increasing complexity and converged to the identification of three local minima on the potential energy surface. To avoid finite size effects along the polymer direction, we then built periodic boxes out of these three structures that were subjected to further structural refinements. These helices, hereafter referred to as h1, h2 and h3, differ by the relative orientation of the PDI chromophores with respect to the main axis of the polyisocyanide backbone (**Fig. 8**). In h1 the PDI are oriented with their long axis forming an angle of ~60° with the helical direction; this is an open structure that shows the lowest density among the three helical arrangements. In contrast, h3 presents a much more compact, pine tree like structure with the PDI chromophores lying

almost down on the helical core (the average angle between the PDI main axis and the helix direction is 26°). A similarly dense structure is achieved in h2 compared to h3, although (in contrast to h1) the chromophores are maintained in an orthogonal orientation (average angle of 94°) with respect to the helical growth direction. From an energetic point of view, the potential energies calculated for these local minima indicate that h3 is the most stable (mostly because of attractive Van der Waals interactions), followed by h2 and h1.

The absolute values of the INDO[43] transfer integrals computed for all possible nearest neighbor pairs in the 4 stacks of each helical conformation are shown on **Fig. 8** for the three structures (h1, h2 and h3); the corresponding averaged values are reported in **Table 1**. At 0K, h1 features a high amount of structural order as clearly illustrated from the almost constant $t_{\perp}$, values across the whole stack. However, molecular dynamics (MD) simulations at room temperature lead to considerable structural disorder, which translates into a broader distribution of transfer integrals along the helical structures. h2 and h3 also display significant fluctuations in the electronic couplings around an average value of ~350 cm^{-1}. Compared to single crystals of small molecules such as the oligoacenes,[44] this is a significant value that should allow for efficient *intramolecular* electron transport along the polymer direction. The sizeable transfer integrals, despite the unfavorable rotation angle (*vide infra*), arise from the close packing of the PDI units.

The systems investigated here present an additional interesting feature. The conformation of the central polyisocyanide backbone is such that all the carbonyl moieities participating to the H-bonding network align along the same direction. This can be better appreciated from **Fig. 9a** showing the ground-state charge distribution, as computed at the INDO level, for a representative stack. As a result, the chromophores in the helical structures experience a local

intramolecular electric field that promotes the formation of a step-like electronic structure, **Fig. 9b**. Thus, these systems should be characterized by interesting rectification properties, since charge motion would occur with different rates along or opposite to the internal field. More work is in progress to study such effects, both theoretically and experimentally. Note also that the presence of the field induces an almost complete localization of the molecular orbitals on individual PDI molecules (because of the resulting energetic disorder), so that a hopping mechanism is at play as anticipated above.

It is of interest to study in more depth the influence of the relative orientation of the chromophores on the electronic coupling values. For this purpose, we have performed a systematic study of the (LUMO) transfer integral in a PDI cofacial dimer with an intermolecular separation of 3.5 Å (consistent with the Dreiding results) along the packing axis Z. A 2D grid has been built by translating one molecule in the XY plane with respect to the second PDI dye. Displacements along axes X and Y (corresponding to the PDI short and long axes, respectively) spanning a range from 0 Å to 5Å with a 0.1Å step have been considered. The calculations were performed for four different values of the rotation angles between the two PDI main axes (ϕ=0°, 10°, 20° and 30°). For the sake of illustration, the electron transfer integrals computed at the INDO level for all possible dimers generated with rotation angles of 0° and 20° are reported as contour plots in **Fig. 10a**. Large variations of $t_{\perp}$ over one to two orders of magnitude are found in the explored range of displacements, which results from the high sensitivity of electronic interactions with the relative spatial positioning of the chromophores and can be traced back to the overlap between the molecular (LUMO) wavefunctions. Of particular interest is the dramatic decrease in transfer integral with rotation angle (**Fig. 10b**); For superimposed molecules (no translation in the XY plane), $t_{\perp}$ surges from a few hundred wavenumbers in the case ϕ=20° (which is the typical value encountered in the

structures generated from the Dreiding MD simulations) to a few thousands wavenumbers for ϕ=0°. Clearly, molecular design rules leading to supramolecular structures with a reduced rotation angle between the electron transport units should be explored for the achievement of molecular wires with improved charge carrier mobilities; these are currently being investigated.

4. Conclusion

The electrical and electronic-transport properties of three different helical multichromophoric arrays have been tested in a comparative study. When polyisocyanopeptides are functionalized with perylene units which are able to interact with each other by π-π stacking (molecule P3), favourable changes in the polymer structure and electronic properties are observed both in solution and on substrates. In general, the π-π interactions are responsible for stronger intermolecular interactions, producing formations of continuous networks of bundles on surfaces and efficient charge transport in thin-film transistors, as demonstrating by comparison with a reference molecule in which the π-π interactions are suppressed due to steric hindrance. The P3 molecule exhibits both fiber formation and *n-type* electroactivity, with carrier mobilities of order 10^{-3} cm^2/Vs at 350K, which are limited by inter-chain transport processes. Issues such as contact-resistance and charge injection, represent interesting challenges in terms of future device optimisation. The WF measurements obtained by KPFM are in satisfactory agreement with previous measurements and with the electrochemical measurements of HOMO and LUMO levels from cyclic voltammetry. Polymer P3 showed a much higher WF than either the polymer without perylenes or the polymer with phenoxy substituents in the perylenes.

The overall approach of attaching individual chromophores to a well defined polymeric scaffold to study their properties and interactions in a situation of reduced degrees of freedom can be applied to the study of many different kinds of small chromophores and presents new ways in which interacting chromophores may be arranged and orientated, due to the presence of the macromolecular "scaffolding" of the backbone. Theoretical modeling of chromophoric interactions in such a helical system confirms the efficiency with which charges may be transported along such structures, as well as suggesting more novel properties, such as rectification due to the internal dipole of the molecule. Together with the ubiquitous nature of the chemical synthesis techniques employed, these studies point towards the further development of innovative supramolecular materials with precisely tailored functionalisation[45] (e.g. heterogeneous chromophoric arrays and donor/acceptor dyad arrays) for optoelectronics applications, such as in photovoltaics.[46]

Received: ((will be filled in by the editorial staff))
Revised: ((will be filled in by the editorial staff))
Published online: ((will be filled in by the editorial staff))

[1] R. van Hameren, P. Schön, A.M. van Buul, J. Hoogboom, S.V. Lazarenko, J.W. Gerritsen, H. Engelkamp, P.C.M. Christianen, H.A. Heus, J.C. Maan, T. Rasing, S. Speller, A.E. Rowan, J.A.A.W. Elemans and R.J.M. Nolte, Science **314**, 1433 (2006)

[2] V. Palermo and P. Samorì, Angew. Chem. Int. Ed. **46**, 4428 (2007)

[3] F. Cacialli, J.S. Wilson, J.J. Michels, C. Daniel, C. Silva, R.H. Friend, N. Severin, P. Samorì, J.P. Rabe, M.J. O'Connell, P.N. Taylor and H.L. Anderson. Nature Mater. **1,** 160 (2002)

[4] T-Q. Nguyen, R. Martel, M. Bushey, P. Avouris, A. Carlsen, C. Nuckolls and L. Brus, Phys. Chem. Chem. Phys. **9**, 1515 (2007)

[5] M. Cavallini, F. Biscarini, S. Léon, F. Zerbetto, G. Bottari and D.A. Leigh, Science **299**, 5606 (2003)

[6] E. Kim, Y. Xia and G.M. Whitesides, Nature **376**, 581 (2002)

[7] Y. Yang, Q. Pei and A. J. Heeger, Appl. Phys. Lett **79**, 934 (1996)

[8] R.H. Friend, R.W. Gymer, A.B. Holmes, J.H. Burroughes, R.N. Marks, C. Taliani, D.D.C. Bradley, D.A. Dos Santos, J.L. Brédas, M. Lögdlund and W.R. Salaneck, Nature **397**, 121 (1999)

[9] H. Sirringhaus, P.J. Brown, R.H. Friend, M.M. Nielsen, K. Bechgaard, B.M.W. Langeveld-Voss, A.J.H. Spiering, R.A.J. Janssen, E.W. Meijer, P. Herwig and D.M. de Leeuw, Nature **401**, 685 (1999)

[10] M. Muccini, Nature Mater. **5**, 605 (2006)

[11] C.W. Sele, T. von Werne, R.H. Friend and H. Sirringhaus, Adv. Mater. **17**, 997 (2005)

[12] C.J. Brabec, N.S. Sariciftci and J.C. Hummelen, Adv. Func. Mater. **11**, 15 (2001)

[13] G. Yu, J. Gao, J.C. Hummelen, F. Wudl and A.J. Heeger, Science **270**, 1789 (1995)

[14] J.J.M. Halls, C.A. Walsh, N.C. Greenham, E.A. Marseglia, R.H. Friend, S.C. Moratti and A.B. Holmes, Nature **376**, 498 (1995)

[15] J.J.L.M. Cornelissen, J.J.J.M. Donners, R. de Gelder, W.S. Graswinckel, G.A. Metselaar, A.E. Rowan, N.A.J.M. Sommerdijk and R.J.M. Nolte, Science **293**, 676 (2001)

[16] J.J.L.M. Cornelissen, W.S. Graswinckel, P.J.H.M. Adams, G.H. Nachtegaal, A.P.M. Kentgens, N.A.J.M. Sommerdijk and R.J.M. Nolte, J. Polym. Sci. A; Pol. Chem. **39**, 4255 (2001)

[17] P.A.J. de Witte, M. Castriciano, J.J.L.M. Cornelissen, L.M. Scolaro, R.J.M. Nolte and A.E. Rowan, Chem. Eur. J. **9**, 1775 (2003)

[18] E. Schwartz, V. Palermo, C.E. Finlayson, Y-S. Huang, M.B.J. Otten, A. Liscio, S. Trapani, I. González-Valls, P. Brocorens, J.J.L.M. Cornelissen, K. Peneva, K. Müllen, F. Spano, A. Yartsev, S. Westenhoff, R.H. Friend, D. Beljonne, R.J.M. Nolte, P. Samorì and A.E. Rowan, submitted (2008)

[19] P. Samorí, C. Ecker, I. Gössl, P.A.J. de Witte, J.J.L.M. Cornelissen, G.A. Metselaar, M.B.J. Otten, A.E. Rowan, R.J.M. Nolte and J.P. Rabe, Macromolecules **35**, 5290 (2002)

[20] D.M. Vriezema, J. Hoogboom, K. Velonia, K. Takazawa, P.C.M. Christianen, J.C. Maan, A.E. Rowan and R.J.M. Nolte, Angew. Chem. Int. Ed. **42**, 772 (2003)

[21] J. Hernando, P.A.J. de Witte, E.M.H.P van Dijk, J. Korterik, R.J.M. Nolte, A.E. Rowan, M.F. García-Parajó and N.F. van Hulst, Angew. Chem. Int. Ed. **43**, 4045 (2004)

[22] P. de Witte, J. Hernando, E.E. Neuteboom, E.M.H.P. van Dijk, S.C.J. Meskers, R.A.J. Janssen, N.F. van Hulst, R.J.M. Nolte, M.F. Garcia-Parajo and A.E. Rowan, J. Phys. Chem. B, **110**, 7803 (2006)

[23] R.E. Blankenship, *Molecular Mechanisms of Photosynthesis* (Blackwell, UK, 2001)

[24] I.H. Campbell, S. Rubin, T.A. Zawodzinski, J.D. Kress, R.L. Martin, D.L. Smith, N.N. Barashkov and J.P. Ferraris, Phys. Rev. B **54**, 14321 (1996)

[25] R.W.I. de Boer , M.E. Gershenson, A.F. Morpurgo and V. Podzorov, Phys. Stat. Sol. (a) **201**, 1302 (2004)

[26] L. Bürgi, H. Sirringhaus and R.H. Friend, Appl. Phys. Lett. **80**, 2913 (2002)

[27] L.Chua, J. Zaumseil, J-F. Chang, E.C-W. Ou, P.K-H. Ho, H. Sirringhaus and R.H. Friend, Nature **434**, 194 (2005)

[28] S. Cho, K. Lee, J. Yuen, G. Wang, D. Moses, A.J. Heeger, M. Surin and R. Lazzaroni, J. Appl. Phys. **100**, 114503 (2006)

[29] J.A. Merlo and C.D. Frisbie, Phys. Rev. B **108**, 19169 (2004)

[30] R.J. Chesterfield, J.C. McKeen, C.R. Newman, P.C. Ewbank, D.A. da Silva Filho, J-L. Brédas, L.L. Miller, K.R. Mann, and C.D. Frisbie, J. Phys. Chem. B **108**, 19281 (2004)

[31] B. I. Shklovskii and A. L. Efros, *Electronic Properties of Doped Semiconductors* (Springer-Verlag, Berlin, 1984)

[32] H.L. Gomes, P. Stallinga, F. Dinelli, M. Murgia, F. Biscarini, D.M. de Leeuw, T. Muck, J. Geurts and L.W. Molenkamp, Appl. Phys. Lett. **84**, 3184 (2004)

[33] Y-Y. Noh, N. Zhao, M. Caironi and H. Sirringhaus, Nature Nanotechnology **2**, 784 (2007)

[34] Cyclic Voltammetry on thin-films of P3, spin-coated onto Pt electrodes, with a Fe/Fe^{+} reference. Oxidation scan 0.0 to +2.0V, rate 100mV/s, E_{ox} = +1.28V. Reduction scan +1.3V to -1.2V, rate 100mV/s, E_{red} = -0.72V.

[35] J.L. Li, M. Kastler, W. Pisula, J.W.F. Robertson, D. Wasserfallen, A.C. Grimsdale, J.S. Wu and K. Müllen, Adv. Func. Mater. **17**, 2528 (2007)

[36] F. Würthner, Chem. Comm. **2004**, 1564

[37] A. Liscio, V. Palermo and P. Samorì, Adv. Func. Mater. **18**, 907 (2008)

[38] C.W. Struijk, A.B. Sieval, J.E.J. Dakhorst, M. Van Dijk, P. Kimes, R.B.M. Koehorst, H. Donker, T.J. Schaafsma, S.J. Pieken, A.M. van de Craats, J.M. Warman, H. Zuilhof and E.J.R. Sudhölter, J. Am. Chem. Soc., **122**, 11057 (2002)

[39] Y. Olivier, V. Lemaur, J.L. Brédas and J. Cornil, J. Phys. Chem. A, **110**, 6356 (2006)

[40] G. Pourtois, D. Beljonne, J. Cornil, M.A. Ratner and J.L. Brédas, J. Am. Chem. Soc., **124**, 4436 (2002)

[41] V. Lemaur, M.C. Steel, D. Beljonne, J.L. Brédas and J. Cornil, J. Am. Chem. Soc., **127**, 6077 (2005)

[42] S.L. Mayo, B.D. Olafson, W.A.J. Goddard III, J. Phys. Chem., **94**, 8897 (1990)

[43] M.C.Zerner, G.H. Loew, R.F. Kichner and V. Mueller-Wasterhoff, J. Am. Chem. Soc.,**102**,589 (1980)

[44] Y.C. Cheng, R.J. Silbey, D.A. da Silva Filho, J.P. Calbert, J. Cornil and J.L. Brédas, J. Chem. Phys. **118**, 3764 (2003)

[45] P. Samorì, F. Cacialli, H.L. Anderson and A.E. Rowan, Synth. Met. **147**, 1 (2004)

[46] M.B.J. Otten, E. Schwartz, P.A.J de Witte, J.J.L.M. Cornelissen, M.M Wienk, R.A.J. Janssen, R.J.M. Nolte and A.E. Rowan, *Helical Perylene Polymers for Application in Photovoltaic Devices,* **PMSE 440**, ACS National Meeting 231 in Atlanta, GA, USA (2006)

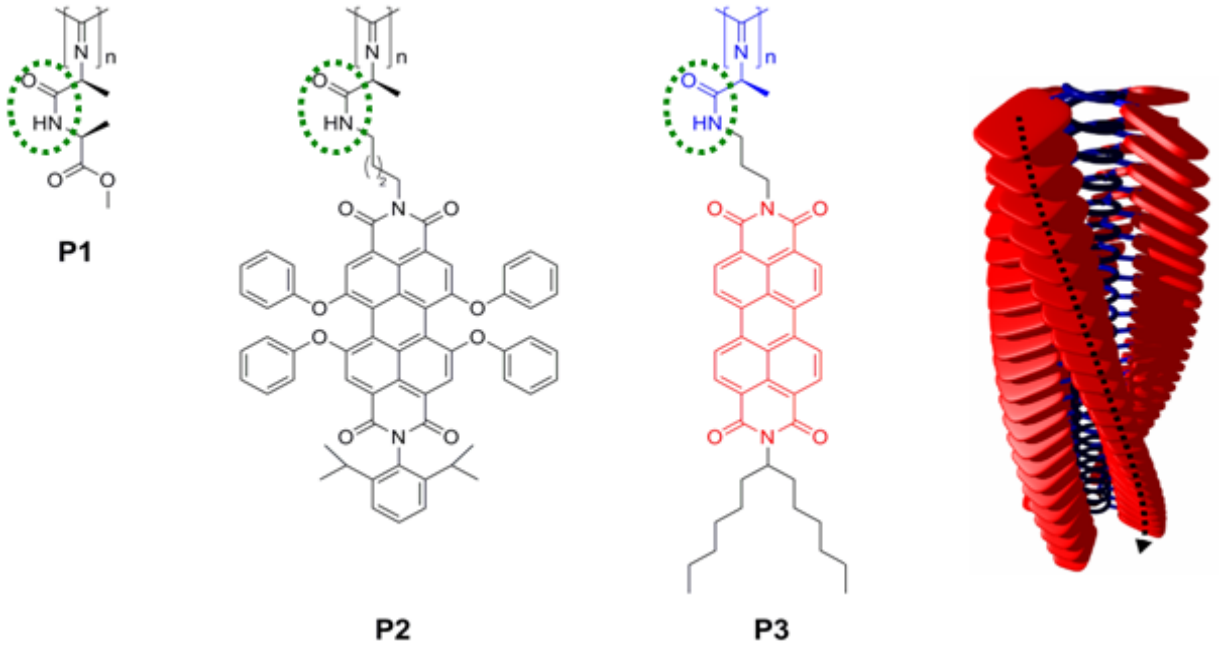

Figure 1. Structure of the three polymers P1, P2 and P3. The amide unit responsible for the hydrogen bonding that stabilizes the helical structure is encircled. A schematic model of the final, coiled structure with side perylene units is also shown.

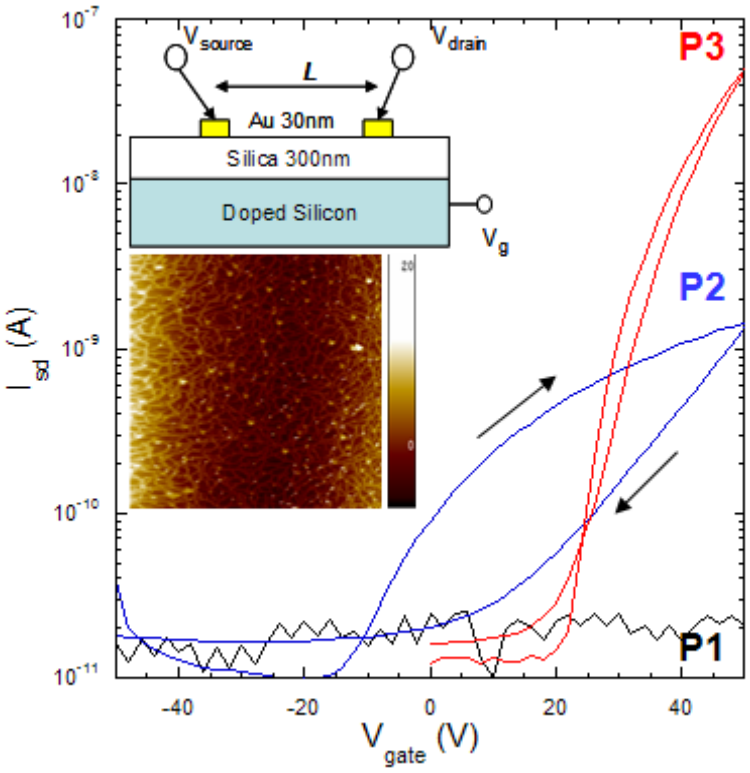

Figure 2. The top inset shows a schematic of the TFT device architecture. The main figure shows transfer characteristics of TFTs of **P1**, **P2** and **P3**, as indicated, with a source-drain bias of 20V and L = 2μm in each case. The gate-voltage sweep direction was from -50V to +50V and then back to -50V, as indicated by the arrows. The lower inset shows a representative AFM image of a network of **P3** deposited into a transistor channel of length ~2 mm. The raised areas toward the edge of the image show where the material is deposited between electrode and channel. The micrograph has an area of 2μm x 2μm and the height scale (0-20 nm) is also shown

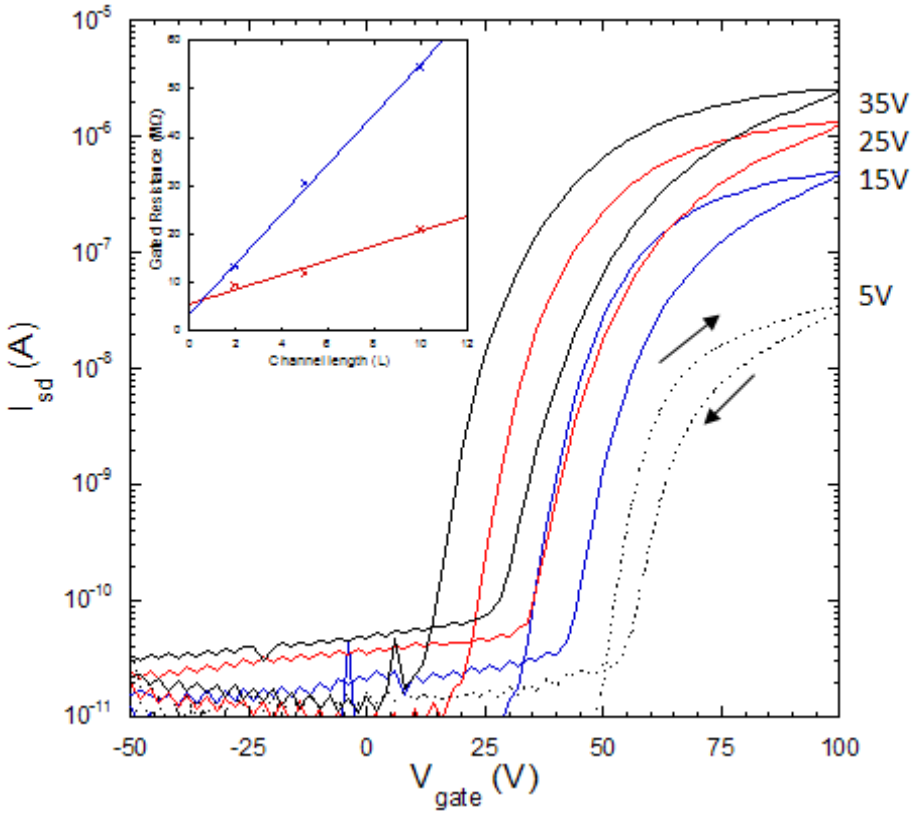

Figure 3. Room temperature transfer characteristics for a TFT (L = 2mm) of **P3**, where the Au electrodes had been pre-treated with a thiol-SAM. The source-drain bias was varied from 5 to 35V, as indicated at the right-hand side of each transfer curve and the measured gate switch-on voltage was +24V. The gate-voltage sweep direction was from -50V to +100V and then back to -50V, as indicated by the arrows. The inset shows the gated resistance $(dV/dI)_{source\text{-}drain}$ of **P3** TFTs vs. device channel length, as measured at a gate voltage of +100V at room temperature. The "as prepared" device (blue) is compared to the behaviour after annealing under N_2 for 1 hr at 150°C (red). This illustrates a reduction in overall film resistance, but little change in the contact resistance, which may be inferred from the value of resistance taken at the y-intercept (L=0).

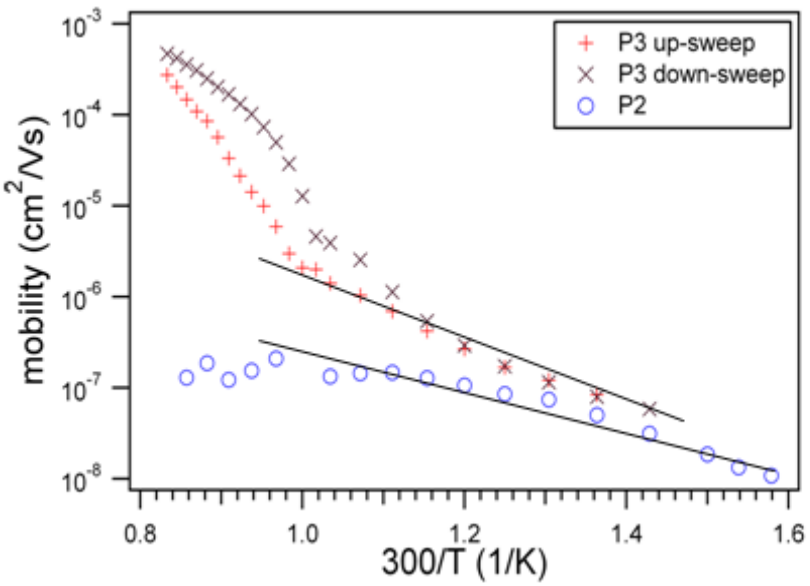

Figure 4. Logarithmic plot of linear-regime mobility as a function of reciprocal temperature for **P3** TFTs (the cycle was down from 360K to 210K [black crosses], then back up from 210K to 360K [red crosses]) and also for **P2** TFTs (blue circles). The lines of best-fit assume a simple Arrhenius behaviour, yielding low temperature activation energies of ε ~200 meV in the case of **P3** and ε ~ 100 meV for **P2**.

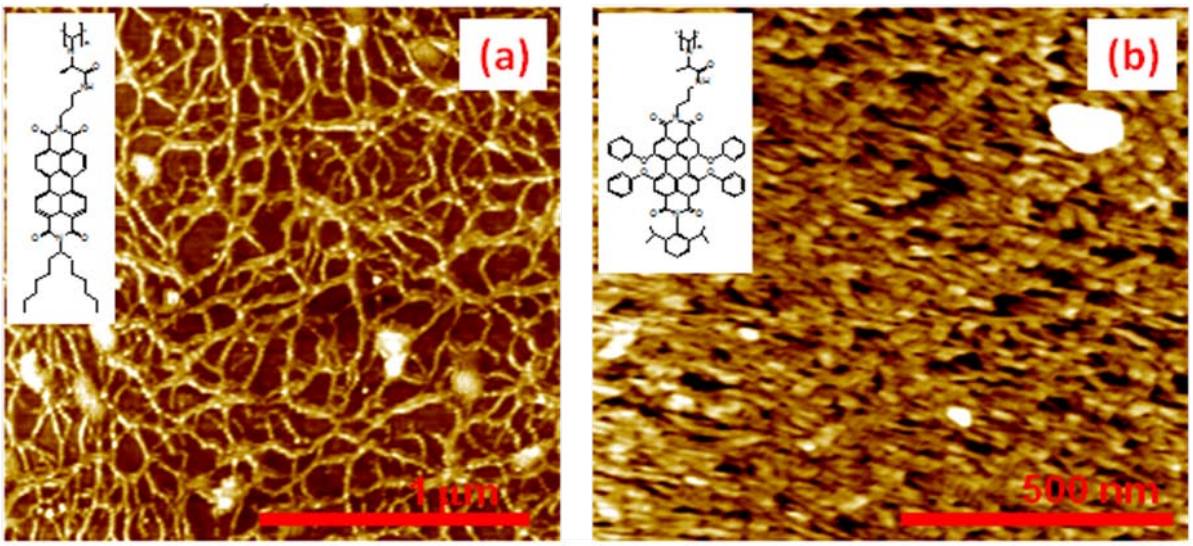

Figure 5: AFM micrographs of continuous, thin layers of **P3** (a) and **P2** (b), spin-coated on SiO_x.

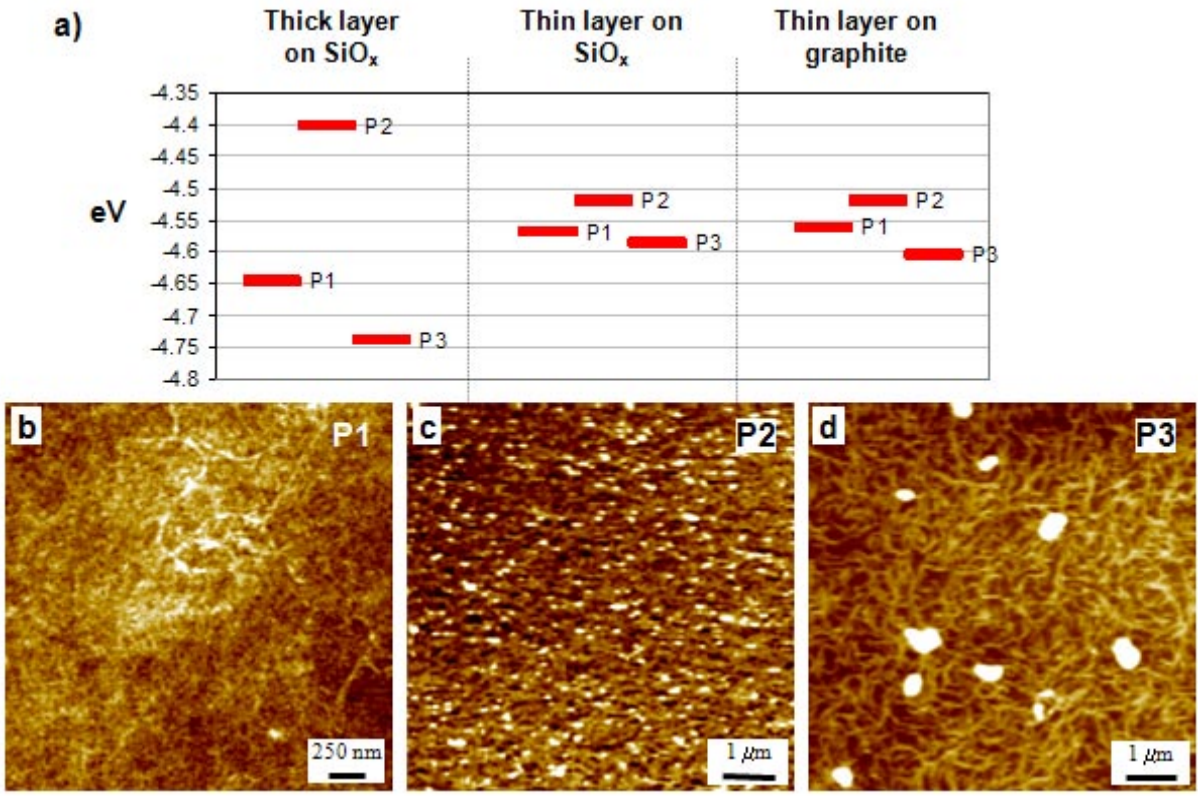

Figure 6: (a) WF of the three molecules, as measured on thick and thin layers on SiOx, and on thin layers on graphite. At low thicknesses, the differences between the molecules are less pronounced. (b,c,d) AFM images of thick layers of **P1**, **P2** and **P3**. Z-ranges are 7, 5 and 8 nm respectively.

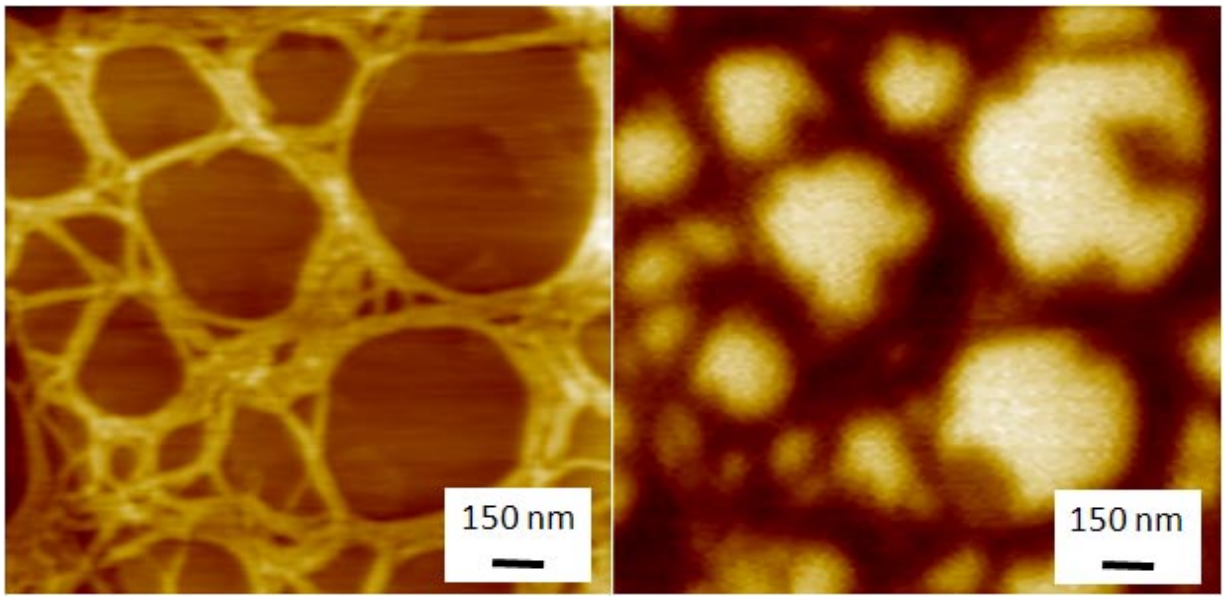

Figure 7. Topography (left) and KPFM image (right) of an ultra thin layer of **P3** molecules on SiOx.

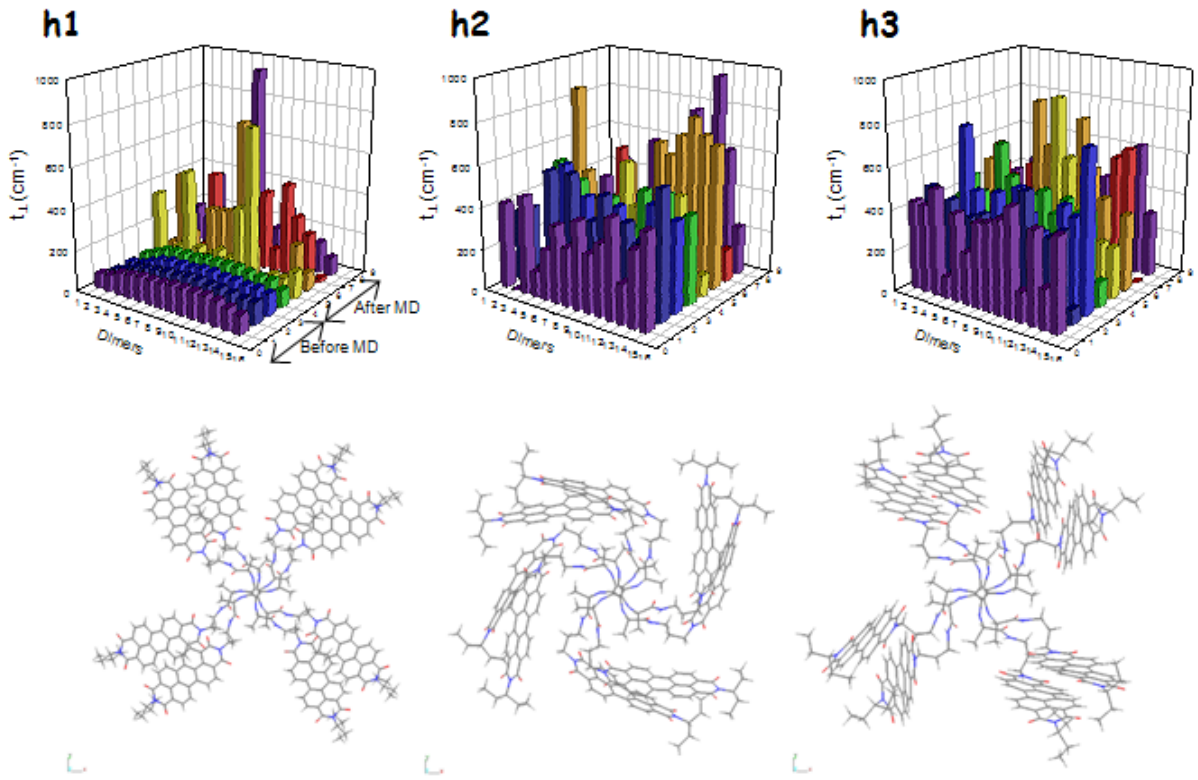

Figure 8. INDO electron (LUMO) transfer integrals for helices **h1**, **h2** and **h3** calculated before (y = 1-4) and after (y = 5-8) the molecular dynamics simulation. Schematic representations of the corresponding geometries of the **P3** molecule used for these simulations are given below

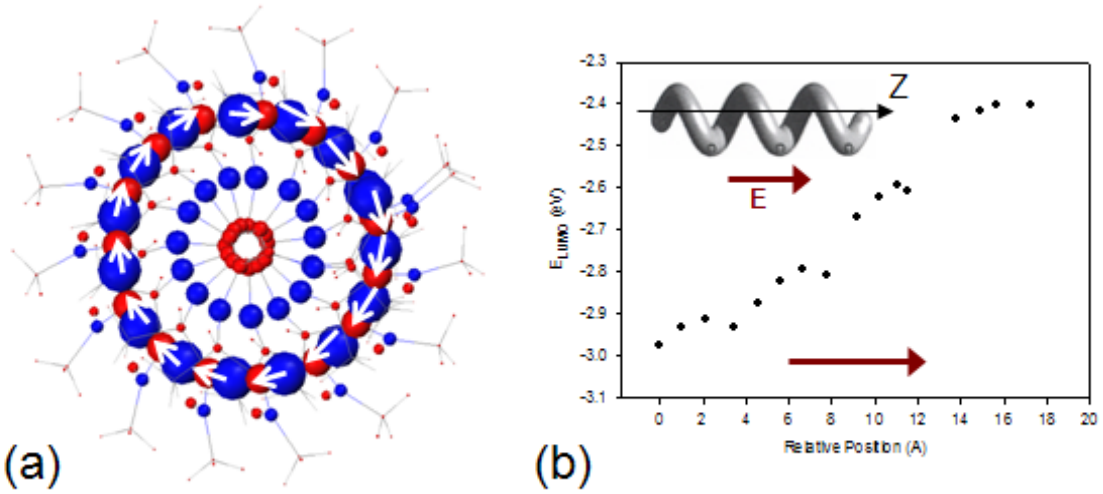

Figure 9. (a) Top view of the polyisocyanide core showing the INDO ground-state charge distribution. White arrows represent local dipoles associated with the C=0 moieities. (b) Energy of the lowest unoccupied molecular orbital (LUMO) computed for helix **h1** at the INDO level as a function of localization along the helical axis

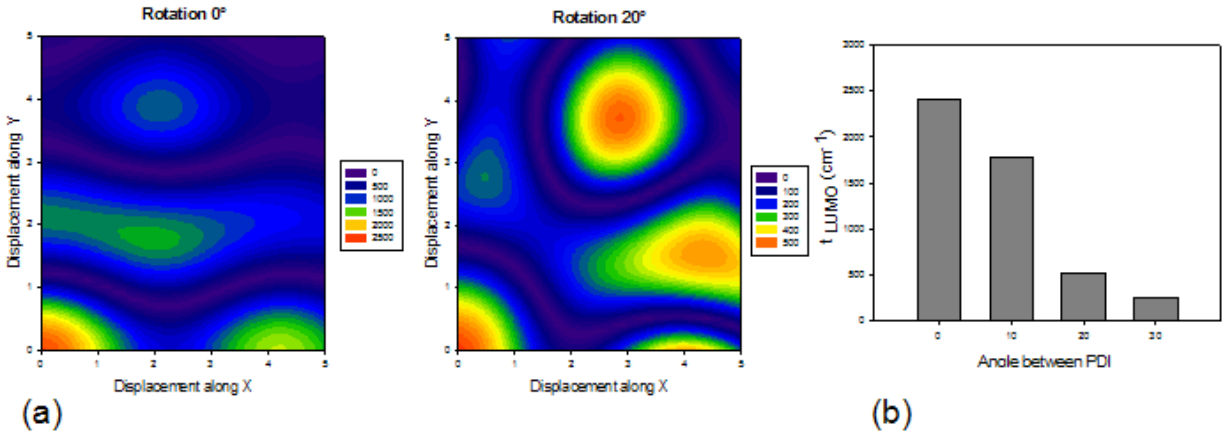

Figure 10. (a) Contour plots of the INDO electron transfer integrals for model dimers constructed by translating in-plane the top molecule with respect to the bottom one, with an intermolecular separation of 3.5Å and rotation angles along the packing direction of 0° and 20°. (b) INDO electron transfer integral as a function of the rotation angle between two superimposed chromophores.

Table 1. Average values and standard deviations of the INDO electron transfer integrals calculated for nearest neighbours in helical structures **h1**, **h2** and **h3** (a) before and (b) after a molecular dynamics simulation.

(a)

Transfer Integral, $t_\perp$ (cm^{-1})

	$< t_\perp >$	$[< t_\perp^2 > - < t_\perp >^2]^{1/2}$
h1	110	21
h2	319	161
h3	376	152

(b)

Transfer Integral, $t_\perp$ (cm^{-1})

	$< t_\perp >$	$[< t_\perp^2 > - < t_\perp >^2]^{1/2}$
h1	196	203
h2	344	213
h3	354	202

Submitted to ADVANCED FUNCTIONAL MATERIALS

The electronic transport properties of perylene-substituted polyisocyanopeptides are studied using thin-film transistors (TFTs). Carrier mobilities of order 10^{-3} cm^2/Vs at 350K are obtained, as limited by inter-chain transport processes. The influence of π-π interactions on the electronic and the electronic-transport properties of these systems are further investigated using Kelvin Probe Force Microscopy (KFPM) and a theoretical study of electronic coupling.

Molecular Electronics

C. E. Finlayson*, R. H. Friend, M. Otten, E. Schwartz, R. Nolte, J. J. L. M. Cornelissen, A. E. Rowan, P. Samorì, V. Palermo, A. Liscio, K. Peneva, K. Müllen, S. Trapani, D. Beljonne,
■<B>…<B>■

Electronic transport properties of ensembles of perylene-substituted poly-isocyanopeptide arrays

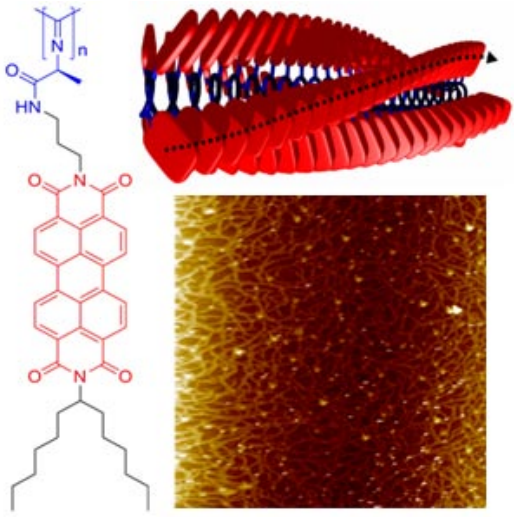

Column Title: *C.E. Finlayson et al.*/ Electronic transport in poly-isocyanopeptide arrays